Macromolecules
ARTICLE

Macromolecules **2010**, *43*, 4149–4160 **4149**
DOI: 10.1021/ma100201g

Crystallization Kinetics and Morphology of Biodegradable Double Crystalline PLLA-*b*-PCL Diblock Copolymers

Reina Verónica Castillo

Laboratorio de Polímeros, Centro de Química, Instituto Venezolano de Investigaciones Científicas IVIC, Apartado 20632, Miranda 1020-A, Venezuela

Alejandro J. Müller*

Grupo de Polímeros USB, Departamento de Ciencia de los Materiales, Universidad Simón Bolívar, Apartado 89000, Caracas 1080-A, Venezuela

Jean-Marie Raquez and Philippe Dubois

Center of Innovation and Research in Materials & Polymers CIRMAP, Service des Matériaux Polymères et Composites SMPC, Université de Mons-UMONS, Place du Parc 20, B-7000 Mons, Belgium

Received January 26, 2010; Revised Manuscript Received March 10, 2010

ABSTRACT: The crystallization kinetics and morphology of biodegradable and double crystalline poly(L-lactide)-*b*-poly(ε-caprolactone) diblock copolymers (PLLA-*b*-PCL) was studied in a wide composition range by differential scanning calorimetry (DSC) and polarized light optical microscopy (PLOM). The two blocks were found to be partially miscible according to the variations of their thermal transitions with composition. PLOM results showed that PLLA crystallizes in a wide composition range with a spherulitic superstructural morphology. Only when the PLLA content is as low as 10 wt % are axialites formed. These results were in good agreement with the overall crystallization kinetics obtained by DSC isothermal experiments and analyzed by the Avrami equation. Both overall crystallization rates and spherulitic growth rates of the PLLA block decrease with PCL content because PCL acts as a diluent for the PLLA block in view of their miscibility. Reorganization processes revealed as double melting peaks for the PLLA block (not observed for the PLLA homopolymer) were observed during heating scans performed after isothermal crystallization. The reorganization ability of the PLLA block was found to increase with PCL content, a fact that quantified the perturbation caused by molten PCL block chains during the isothermal crystallization of the PLLA block. The PCL block crystallizes within previously formed PLLA spherulites or axialites. Despite the partial miscibility, unexpected and novel fractionated crystallization of the PCL occurs at contents of PCL between 40 and 19 wt %. For the lowest PCL content (i.e., 19%), a homogeneous nucleation process was detected, as indicated by the large supercooling needed for crystallization and by the first-order crystallization kinetics obtained (i.e., Avrami index close to 1). Because of the partial miscibility, the glass-transition temperature of the PLLA block ($T_{g,PLLA}$) decreases with PCL addition, so at PCL contents lower than 40 wt %, the $T_{g,PLLA}$ values are close to or higher than the crystallization temperature of the PCL block. Therefore, PCL fractionated crystallization is induced by hard confinement of the PLLA amorphous and crystalline regions. This is the first time that a homogeneous nucleation process has been documented for a crystallizable component in a miscible or weakly segregated diblock copolymer. The PCL block can also be nucleated by previously formed PLLA crystals depending on the crystallization degree of the PLLA, which was varied by self-nucleation experiments. The crystallization rate of PCL strongly decreased with increasing PLLA content.

Introduction

Many interesting aliphatic polyesters are biodegradable and biocompatible materials.[1] Among them, poly(L-lactide) (PLLA) has been widely employed in the industrial and medical field because of its high-strength, high-modulus, and biocompatibility.[2,3] Poly(ε-caprolactone) (PCL) is a highly processable biopolymer that can be hydrolytically or enzymatically degraded, having therefore large applications in various areas such as medicine and agriculture.[4,5] PLLA and PCL have attracted increasing attention in the pharmaceutical and medical fields for potential uses as bioresorbable sutures, orthopedic fixation devices, artificial skin, tissue engineering scaffolds, and drug delivery systems because their biodegradation in physiological conditions yields nontoxic products that can be bioabsorbed or excreted by the human body.[1,2]

Even though PLLA exhibits relatively good mechanical properties, its commercial products are limited by its brittleness and stiffness. PCL exhibits a low glass-transition temperature (−60 °C), remarkable drug permeability,[6] and elasticity but very low degradation rates due to the fairly high crystallinity. Therefore, copolymerization or blending of PLLA with PCL could allow the fabrication of a variety of biodegradable materials with improved properties in comparison with those of the parent homopolymers. Nevertheless, high-molecular-weight PLLA/PCL blends are reported to be immiscible,[7−10] and thus desirable mechanical properties for specific applications may not be anticipated. If block

*Corresponding author. E-mail: amuller@usb.ve.

Published on Web 04/09/2010

copolymers of PLLA-*b*-PCL are produced, then macrophase separation is avoided and a better control on the composition and morphology can be obtained.[3]

Block copolymers can self-assemble in the melt into a diversity of ordered structures with nanoscale periodicities via microphase separation. These structures can be controlled by varying the composition of the block copolymer or the segregation strength between blocks. Therefore, we can tailor the copolymer properties to meet the requirements of various applications by varying the copolymer composition, monomer sequencing, and molecular weight.[11] The mechanical properties as well as biodegradability are also very much affected by the crystallinity of the constituent blocks that in turns depends on microdomain structure. Therefore, crystallization is an important process to determine the application of a semicrystalline block copolymer. The overall crystallinity is also influenced by the nucleation type, the crystallization kinetics, and the characteristic of the individually folded chains.[12,13] Therefore, it is expected that the solid-state structure including the crystalline lamellar organization plays an important role in controlling the kinetics of bioabsorption. The study on the crystallization is thus of great importance not only for academic interest but also from the engineering viewpoint.[14]

The subject of crystallization in block copolymers has attracted much attention, and several reviews have recently been published.[14−19] Another recent review deals specifically with crystallization in biodegradable or biostable block copolymers.[12] Crystallization can be confined within the copolymer microdomain structure for strongly segregated systems, or it can drive structure formation for weakly segregated melts (overwriting any previous microdomain structure) or homogeneous systems. In the case of double crystalline diblock copolymers, the situation can be even more complicated because the crystallization of one block may affect the crystallization and morphology of the second block. In fact, the second block could be nucleated, or its crystallization could be confined within the microdomain structure or within the previously formed lamellar stacks of the first block. Confined crystallization can lead to fractionated crystallization. The fractionated crystallization phenomenon has been explained as the crystallization of a series of microdomains at specific and independent supercoolings, that is, the crystallization of the isolated domains of a semicrystalline polymer dispersed in an immiscible matrix, where the number of domains is higher than the number of active heterogeneous nuclei. Therefore, the different groups of domains may contain distinct type of heterogeneities with diverse efficiency to induce nucleation or even can contain no heterogeneity at all, and thus they will crystallize at different supercoolings.[17] Few published works have reported fractionated crystallization in miscible systems.[20−22] He et al.[20] first reported fractionated crystallization and even homogeneous nucleation for miscible blends of poly(ethylene oxide)/poly(butylene succinate). In addition, Castillo and Müller[12] reported that fractionated crystallization can be present in miscible PEO-*b*-PCL block copolymers. In these cases, one of the components is able to crystallize at much higher temperatures than the second component. During the crystallization of the first component, spherulites are formed, and the second component remains in the melt. Upon further cooling, the crystallization of the second component occurs in a confined fashion within the interlamellar regions of the first component. Nevertheless, homogeneous nucleation in miscible block copolymers has not been reported as far as the authors are aware.

The double-crystalline PLLA-*b*-PCL diblock copolymers have been reported as miscible or weakly segregated in the melt, depending on composition and molecular weight.[23−29] A previous work and a review recently published summarize our findings on the melt morphology of these materials (ref 28, see also Table 2 from ref 12). We have previously investigated[27,28] the crystallization of three well-defined PLLA-*b*-PCL diblock copolymers by time-resolved X-ray techniques, polarized light optical microscopy (PLOM), and differential scanning calorimetry (DSC). Three compositions were studied that contained 32, 44, and 56 wt % PLLA. The copolymers appear to be initially miscible in the melt; however, detailed evaluation by time-resolved SAXS experiments indicated that the samples with 44 and 56 wt % crystallize from microphase-separated structures, whereas the sample with 32 wt % crystallizes from a homogeneous melt. For the melt-segregated samples, a lamellar structure with a different periodicity than that obtained in the melt forms, as indicated by SAXS. Isothermal experiments at two crystallization temperatures showed that the crystallization rate of PLLA decreased with PCL content. Finally, PLLA negative spherulites formed regardless of composition. The miscibility of the amorphous phase in a wide composition range for the PLLA-*b*-PCL systems was studied by Laredo et al.[29] using thermally stimulated depolarization currents technique (TSDC); the systems were found to be miscible with multiple glass transitions because of distinct segmental mobilities in the amorphous phase.

Although these systems have been previously evaluated[30−35] and morphological studies have been previously performed by SAXS,[24,27,28] a detailed study of the crystallization kinetics and morphology of both blocks, and their dependence with composition in a wide range has not been reported, as far as we are aware. In this work, we report the overall crystallization kinetics, the melting behavior after isothermal crystallization, spherulitic growth rate, and morphology of both PLLA and PCL blocks within PLLA-*b*-PCL diblock copolymers, employing DSC and PLOM. Also, novel results of homogeneous nucleation in miscible block copolymers are reported. We present experimental data illustrating how the isothermal crystallization behavior of both PLLA and PCL blocks can be affected by being covalently linked in a block copolymer,

The understanding of the complicated properties of double-crystalline diblock copolymers is still in a nascent stage despite the number of prior reports that have been published.[36−41] Therefore, the PLLA-*b*-PCL block copolymers can be excellent models to study how these properties change on miscible or weakly segregated systems compared with their parent homopolymers. Moreover, complex competitive effects are present in these systems, such as miscibility and weak segregation depending on composition; and crystallization and microphase separation; and crystallization of the PCL block under hard or soft confinement because the T_g of the PLLA block may be higher or lower than the crystallization temperatures of the PCL block depending on composition.

Experimental Section

Poly(L-lactide)-*b*-poly(ε-caprolactone) diblock copolymers were synthesized by controlled/"living" sequential block copolymerization, as initiated by aluminum trialkoxides in toluene solution. These procedures were previously reported in detail.[27,42] Table 1 lists the molecular weight characterization data obtained by size exclusion chromatography (SEC) and by ^{1}H NMR. The diblock nomenclature that we have used denotes the PLLA block as L and the PCL block as C, subscripts indicate the approximate composition in wt %, and superscripts indicate the approximate number-average molecular weight of the entire block copolymer in kilograms per mole.

Differential Scanning Calorimetry. A Perkin-Elmer DSC-7 power compensated differential scanning calorimeter was employed. Samples with ∼5 mg in weight were encapsulated in aluminum pans. The calibration was performed with indium and hexatriacontane and an ultra pure nitrogen atmosphere was employed as circulating atmosphere for all tests. Measurements during cooling and heating at 10 °C/min as well as in isothermal

Table 1. Molecular Characteristic of the Block Copolymers and Homopolymers

sample	PLLA/PCL exptl comp[a]	$M_{n,exptl}$ (kg/mol) PLLA block[b]	$M_{n,exptl}$ (kg/mol) PCL block[c]	I[d]
$PLLA^{24}$	100/0	23 900		1.1
$L_{93}C_{07}{}^{18}$	93/07	15 700[e]	1700[e]	1.3
$L_{81}C_{19}{}^{21}$	81/19	16 700[e]	3900[e]	1.3
$L_{60}C_{40}{}^{21}$	60/40	12400	8500	1.1
$L_{55}C_{45}{}^{18}$	55/45	9500	8100	1.4
$L_{44}C_{56}{}^{25}$	44/56	11 100	14 200	1.3
$L_{32}C_{68}{}^{22}$	32/68	6900	14 900	1.4
$L_{10}C_{90}{}^{24}$	10/90	2400	21 500	1.4
PCL^{29}	0/100		28 900	1.3

[a] Experimental composition as determined by ^{1}H NMR. [b] Calculated M_n estimated by ^{1}H NMR for the PLLA knowing the M_n of the PCL block determined by SEC. [c] Experimental M_n estimated by SEC for the PCL block. [d] Polydispesrsity index of the final copolymer (determined by SEC). [e] Theorical M_n estimated considering monomers conversion (calculated by gravimetry).

mode were performed. Isothermal crystallization of the PLLA block within the PLLA-*b*-PCL diblock copolymers was performed after melting at 190 °C for 3 min and rapid cooling to the crystallization temperature at 60 °C/min. The samples were crystallized at the isothermal crystallization temperature until saturation and the DSC recorded the crystallization process as a function of time.

To study the isothermal crystallization kinetics of the PCL block within the diblock copolymers, the PLLA block was first crystallized until saturation. The sample was cooled from the melt at 10 °C/min to −20 °C and then heated at the same rate to 110 °C to melt the PCL block fully but not the PLLA block. Then, the sample was annealed at 110 °C for 15 min to promote further crystallization and annealing of the PLLA block. Finally, the sample was cooled at 60 °C/min to the chosen crystallization temperature of the PCL block, and the isothermal crystallization was recorded by DSC.

Isothermal step crystallizations (ISC) experiments for the PCL block within $L_{81}C_{19}{}^{21}$ diblock copolymer were employed, and the detailed procedure, based on ref 43, is explained as follows. The PLLA block was first crystallized until saturation, as explained above. The sample was cooled and later melted to 80 °C for 3 min. Then, it was quenched from the melt (at 60 °C/min) to the first crystallization temperature, T_{c1}, and it was held at this temperature for a given crystallization time, t_1. Then, the sample was heated from T_{c1} to 80 at 10 °C/min. The heat of fusion was determined, and it was assumed to be equal to the heat of crystallization evolved during the isothermal crystallization step applied at t_1. The procedure was repeated successively for different isothermal crystallization times until enough data were collected to determine the isothermal crystallization kinetics at T_{c1}. Then, another crystallization temperature was chosen, and the whole process was repeated at different times.

High-speed DSC was performed in a Perkin-Elmer Pyris 1. To minimize reorganization phenomena during heating, heating scans at 80 °C/min after isothermal crystallization were employed, as was reported by Pijpers et al.[44] To avoid as much as possible thermal lag (superheating effects), the sample mass was reduced (from 5 to 0.63 mg) in the same factor that the scan rate was increased (from 10 to 80 °C/min). The experiments were performed in a DSC without any modification, so the linearity of the temperature−time relationship during the measurement (during heating) was confirmed by employing the software of the DSC to make sure that heating rates were accurate.

Self-nucleation experiments were performed to the PLLA block. Details of the experimental method can be found in previous works.[45−48] The procedure employed was: (i) The samples were heated to a temperature high enough to melt the polymer completely to erase crystalline thermal history. (ii) They were cooled at 10 °C/min to −20 °C to provide them with a standard thermal history. During this standard cooling, the polymer

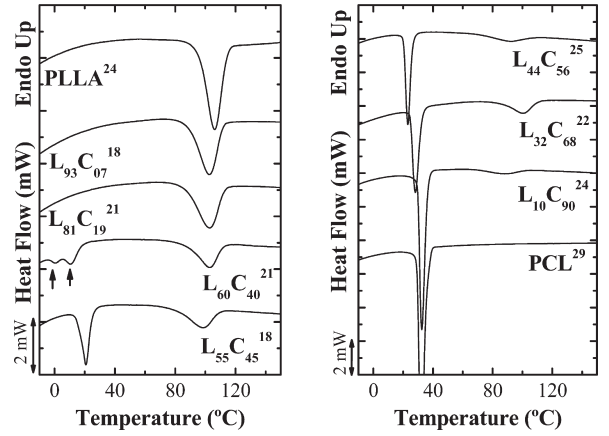

Figure 1. DSC cooling scans at 10 °C/min after melting at 190 °C for 3 min.

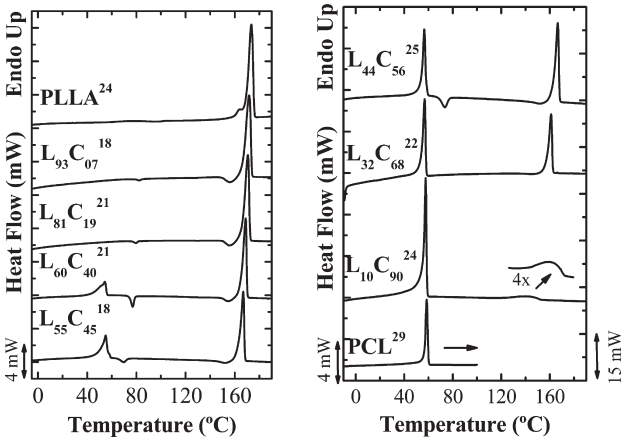

Figure 2. DSC subsequent heating scans (at 10 °C/min) to the cooling scans presented in Figure 1.

crystallized by heterogeneous nucleation. (iii) The samples were heated to a temperature denoted T_s (or self-nucleation temperature) and isothermally kept there for 3 min. (iv) After treatment at T_s, the sample was cooled to −20 °C and (v) subsequently heated at 10 °C/min until melting. Depending on T_s, the sample can be in: Domain I, at high T_s values, the sample is completely molten; Domain II or exclusive self-nucleation domain, when T_s is high enough to melt almost all crystals but low enough to produce self-seeds and therefore the nucleation density can be extremely increased; Domain III or self-nucleation and annealing domain, the sample is partially molten so that self-nucleation and annealing of unmelted crystals take place at T_s.[47]

Polarized Light Optical Microscopy. The superstructural morphology was observed in thin films prepared between microscope coverslips by melting the polymer at 190 °C for 3 min and then quickly cooling to the isothermal crystallization temperature in a Linkam TP-91 hot stage. The samples were observed between crossed polarizers in a Zeiss MC-80 optical microscope equipped with a camera system. To enhance contrast and determine the sign of the spherulites, a λ wave plate was inserted between the polarizers.

Results and Discussion

Standard DSC Results. Figure 1 shows DSC cooling scans and Figure 2 shows subsequent heating scans performed at 10 °C/min for the diblock copolymers and similar molecular weight homopolymers. The observable transition enthalpies and relevant temperatures are reported in Table 2. Figure 1 shows that in general both blocks crystallize during cooling from the melt at lower temperatures than the corresponding

Table 2. Thermal Properties Obtained from DSC Scans Presented in Figures 1 and 2

	PLLA								PCL			
sample	T_c (°C)	T_{cc} (°C)	T_{exo} (°C)	T_m (°C)	ΔH_c (J/g)	ΔH_{cc} (J/g)	ΔH_{exo} (J/g)	ΔH_m (J/g)	T_c (°C)	T_m (°C)	ΔH_c (J/g)	ΔH_m (J/g)
PLLA[24]	106.2	95.9		173.5	48	1		68				
$L_{93}C_{07}$[18]	102.6	82.4	156.0	171.7	38	1	6	62				
$L_{81}C_{19}$[21]	102.8	79.7	155.9	170.5	39	1	6	63				
$L_{60}C_{40}$[21]	102.8	77.0	154.9	168.9	30	8	5	69	0.5−11.3	54.4	18	35
$L_{55}C_{45}$[18]	98.3	69.7	151.9	166.9	29	6	3	69	20.8	55	35	42
$L_{44}C_{56}$[25]	91.8	73.5	151.0	166.5	20	15	2	82	23.2	56.5	44	49
$L_{32}C_{68}$[22]	100.3			161.0	45			75	28.1	56.9	44	45
$L_{10}C_{90}$[24]	86.8			141.5	54			74	32.5	57.7	54	56
PCL[29]									32.2	58.5	69	67

homopolymer. However, the PCL block remains amorphous within $L_{81}C_{19}$[21] and $L_{93}C_{07}$[18], a fact that is confirmed by the lack of melting endotherms corresponding to the PCL block during the subsequent heating scans for these diblock copolymers (see Figure 2). In addition, the PCL block in the $L_{60}C_{40}$[21] diblock copolymer crystallizes in a multiple peak exotherm (pointed by arrows in Figure 1), indicating that fractionated crystallization occurs in this system despite the partial miscibility of the components, as explained in the Introduction. This phenomenon will be treated in detail below when the crystallization of the PCL block will be considered.

The subsequent heating scans presented in Figure 2 show that the thermal behavior of the PLLA block depends on the block copolymer composition. PLLA[24] shows a large well-defined melting peak with a minor low-temperature shoulder. The PLLA blocks within the diblock copolymers with PLLA contents above 32 wt % behave differently. They show two exothermic peaks: one is located at around 69−82 °C (presented in Table 2 as T_{cc}), and the other one appears just before the main melting peak at temperatures around 151−156 °C (see Table 2; this second peak is referred as T_{exo}). At PLLA contents < 32 wt %, no exothermic or additional endothermic peaks are observed besides the main fusion endotherms of PLLA and PCL.

Another interesting observation that can be made from Table 2 and Figure 2 is that the magnitude of the first exothermic signal (ΔH_{cc}) increases with the decrease in PLLA content, whereas the magnitude of the second exothermic peak (ΔH_{exo}) decreases. The exothermic peak located at around 69−82 °C corresponds to cold crystallization of PLLA chains during heating. The one at high temperatures has been previously observed for PLLA homopolymers of different molecular weights during heating scans and has been attributed to recrystallization[49−51] or to the formation of a more stable crystalline phase; see below.[14,52−57] Also, combinations of these mechanisms have been reported depending on molecular weight, crystallization temperature, cooling or heating rates, and melting conditions.[55] Similarly, the melting peak shoulder for PLLA[24] has been explained as a consequence of one or both phenomena.[49,51,55,58]

Zhang et al.[53] showed by real-time FTIR that a more stable α form, referred to as the α′ form (the α form is believed to arise from cold-crystallization or crystallization from the melt), is produced just below the melting point of the PLLA sample when the samples were isothermally crystallized at temperatures below 120 °C. Later, Kawai et al.[14] and Zhang et al.[52] proposed that this α−α′ transformation is a solid−solid phase transition.

The appearance and intensity of the small exotherm observed before the main melting peak have been reported as being dependent on cooling and heating rates.[49,50] This suggests that the initial structure developed during melt crystallization

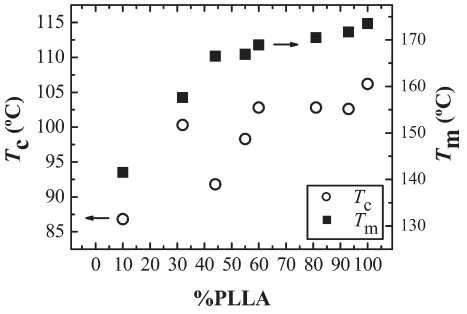

Figure 3. Crystallization and melting temperatures (obtained from the data reported in Figures 1 and 2 and Table 2) for the PLLA block within all copolymers versus PLLA content.

and subsequently cold crystallization can significantly influence the melting behavior of PLLA. The higher the crystallization rates, the more likely it will be for small and imperfect crystals to change successively into more stable crystals through a melt-recrystallization mechanism or by a phase transition, giving rise to the exothermic signal before the melting peak.[49,50] Similar conclusions have been reported for samples isothermally crystallized at low and high temperatures. For the samples crystallized at high temperatures, no such exotherm could be observed.[51,53,59] The reason why the samples studied here exhibit such small exothermic signals and why their magnitude changes with composition is actually unknown, and it is beyond the scope of this article. However, whichever mechanism is taking place during the heating scan of the PLLA block (recrystallization or phase transition), such behavior is influenced by the PCL content in the diblock copolymer.

Figure 3 (and also Table 2) shows how the T_c and T_m values of the PLLA homopolymer and PLLA block within the diblock copolymers (taken from Figures 1 and 2) depend on composition. In general, the crystallization and melting temperature of the PLLA block within the diblock copolymers decrease when the PLLA content decreases. These block copolymer systems have been reported as partially miscible or weakly segregated at compositions closer to symmetric block lengths (with lamellar morphologies), as explained in the Introduction (see also Table 2 from ref 12); therefore, there are two effects in these systems: (1) For extreme compositions, PCL chains can act as a diluent depressing both T_c and T_m of the PLLA block. (2) For symmetric compositions, there are confinement effects within nanodomains induced by microphase separation, which may also reduce T_c or decrease the crystallization rate. However, because of the weak segregation state, a certain level of thermodynamic interactions between the blocks is expected and that allows the PCL to act as a diluent. For weakly segregated systems, break out occurs during crystallization

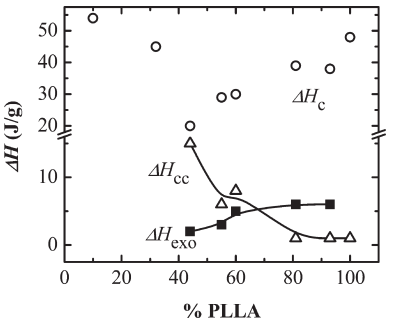

Figure 4. Enthalpies of crystallization (ΔH_c), cold crystallization (ΔH_{cc}), and enthalpy of the exothermic signal prior to melting (ΔH_{exo}) (obtained from the data reported in Figures 1 and 2 and Table 2) for the PLLA block within all copolymers versus PLLA content.

(modifying any preexisting melt morphology), and during heating, the melting behavior would be affected by the miscibility between the blocks. In addition, the crystallization temperature of the PLLA block within the diblock copolymers during the cooling scans is influenced not only by composition but also by the molecular weight and nucleation density. As a result, T_c values of the PLLA block shown in Figure 3 and Table 2 have a large scatter with composition.

T_m values can be strongly affected by molecular weight below a critical value. If we consider T_m values reported in the literature,[55,58,60,61] then this critical value is apparently located at 30−40 kg/mol, and thus both the diluent effect and molecular weight are causing the depression of the melting temperatures of the PLLA block within the diblock copolymers. However, similar diluent effects on the PLLA block have been also observed for miscible PLLA-*b*-PEO systems with increasing PEO composition.[62−64] The crystallization enthalpies during cooling (ΔH_c), the cold crystallization enthalpies during heating (ΔH_{cc}), and the enthalpies of the exothermic signal prior to the main melting peak (ΔH_{exo}) for the PLLA block are plotted in Figure 4.

Figure 4 shows that ΔH_c decreases continuously until the PLLA content reaches 44 wt %; such a decrease is probably due to the diluent effect of the PCL component. However, both $L_{32}C_{68}$[22] and $L_{10}C_{90}$[24] diblock copolymers have higher ΔH_c values (corresponding to the PLLA block) in comparison with the other block copolymers despite the higher PCL content. Because of partial miscibility, the glass-transition temperature (T_g) of the PLLA block decreases with increasing PCL content, as already reported in a previous work.[29] In addition, the PLLA blocks within these systems have very low molecular weights, so both conditions can help the PLLA block to achieve high crystallinity values in $L_{32}C_{68}$[22] and $L_{10}C_{90}$[24]. Because of these high crystallinity values (between 45 and 55%), the PLLA blocks within these two copolymers do not show any crystallization exotherms upon subsequent heating.

It should be noticed that ΔH_{cc} increases as the PLLA content decreases (see Figure 4), whereas at the same time ΔH_c decreases. This is a reflection of the disturbing effect that the molten PCL block can induce on the crystallization of the PLLA block from the melt. As it would be expected, cold crystallization of the PLLA block increases as lower crystallinities were developed.

As previously explained, the exotherm that occurs just before the melting peak of PLLA during the heating scans (Figure 2) is probably due to reorganization or a phase transition. Figure 4 shows that the enthalpy related to this process, ΔH_{exo}, decreases as the PLLA content decreases, a fact probably connected to the simultaneous increase in ΔH_{cc}.

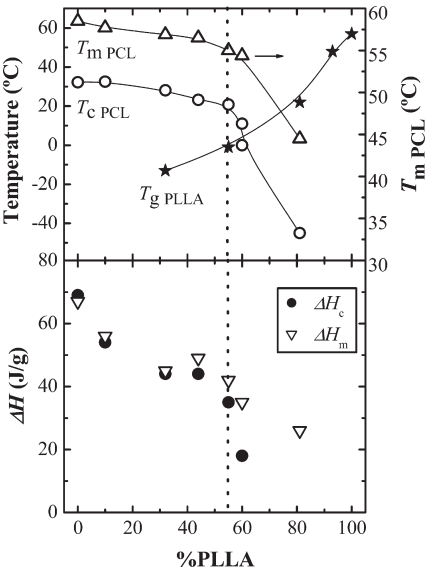

Figure 5. Above: Crystallization and melting temperatures (obtained from the data reported in Figures 1 and 2 and Table 2) corresponding to the PCL blocks and the glass-transition temperature of the PLLA block (data obtained from ref 29) within all copolymers versus PLLA content. Below: Crystallization and melting enthalpies of the PCL block within all copolymers versus PLLA content.

Further studies are required to elucidate the mechanisms that affect such transition prior to the melting of the PLLA block within the PLLA-*b*-PCL diblock copolymers. However, this behavior further suggests that PCL content influences the initial structure developed during the melt crystallization of the PLLA block and its subsequent melting behavior. The melting enthalpy of the PLLA block within the diblock copolymers (see Table 2) remains almost invariable and with higher values than ΔH_c because of the reorganization phenomena that occur during heating, as already reported for PLLA homopolymers crystallized under different conditions.[13]

Turning our attention to the PCL block, its crystallization occurs after the PLLA block crystallization during the cooling scans. Figure 5 shows how T_c, T_m, and enthalpy values of the PCL block, obtained from Figures 1 and 2 (shown in Table 2), vary with composition. The glass-transition temperatures for the PLLA blocks determined by TSDC (from ref 29) were also plotted in Figure 5. As explained above, only one crystallization peak of the PCL block was observed for most of the block copolymer samples. However, at least two crystallization peaks were detected for the $L_{60}C_{40}$[21] block copolymer, suggesting the occurrence of fractionated crystallization. The values of T_c of both peaks for the $L_{60}C_{40}$[21] sample were plotted in Figure 5. In addition, for the $L_{81}C_{19}$[21] block copolymer, PCL chains remain amorphous after being cooled to −20 at 10 °C/min; however, the PCL block was able to crystallize if the sample is cooled to −60 at 10 °C/min, as revealed by the appearance of a melting endotherm in the subsequent heating scan (result not shown). The approximate crystallization temperature and melting temperature for the $L_{81}C_{19}$[21] block copolymer under these special conditions are also reported in Figure 5. The crystallization temperature of the PCL block ($T_{c,PCL}$) within $L_{81}C_{19}$[21] diblock copolymer is located around −45 °C, which can be attributed to the crystallization by previous homogeneous nucleation in view of its very close value to the PCL glass transition.[17,18]

When the PLLA content is low, $T_{c,PCL}$ decreases almost linearly with the decrease in PLLA content. However, it drops quickly at high PLLA content; a similar trend was

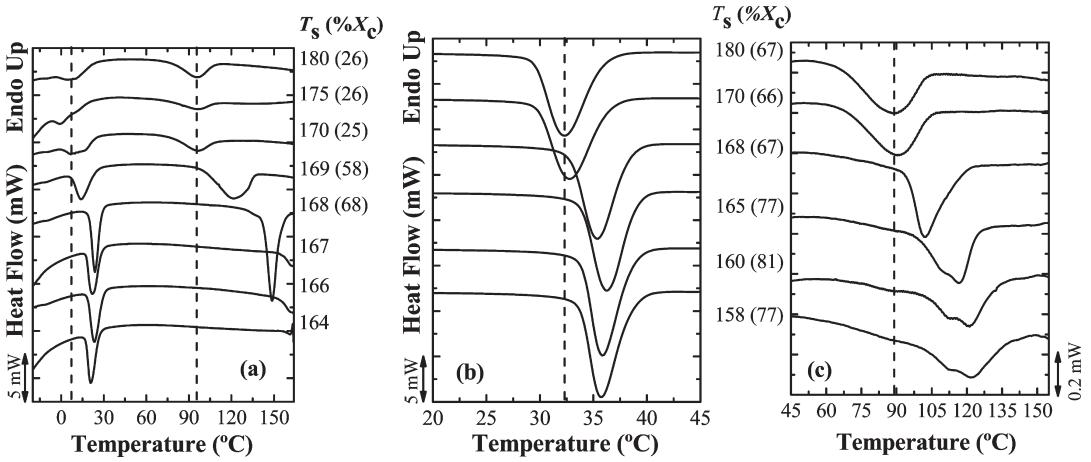

Figure 6. DSC cooling scans at 10 °C/min after self-nucleation of the PLLA block within (a) $L_{60}C_{40}$[21] and (b,c) $L_{10}C_{90}$[24] diblock copolymers at the indicated self-nucleation temperatures (T_s). Part b shows just the PCL crystallization, and part c shows just the PLLA crystallization within $L_{10}C_{90}$[24] diblock copolymer. (See heat flow and temperature scales of the Figures.) The values indicated in brackets correspond to the degree of crystallinity (% X_c) obtained for the PLLA block after self-nucleation.

found with $T_{m,PCL}$. The crossover in behavior occurs at 55 wt % PLLA. The enthalpies of crystallization and melting also decrease with PLLA content (Figure 5). The depressions observed in the values of T_c, T_m, ΔH_c, and ΔH_m of the PCL block are probably related to confinement effects induced by the lamellar stacks of previously crystallized PLLA block chains. In strongly segregated diblock copolymers, the crystallizable block is confined to its small isolated microdomains, and these result in fractionated crystallization. In our case, the PCL chains in the miscible block copolymers with contents of PCL lower than 44 wt % are confined within the interlamellar regions of the previously crystallized PLLA block spherulites. It is interesting to note that sharp decreases in $T_{m,PCL}$ and $T_{c,PCL}$ occur when the PCL block is no longer the majority component. As the PCL chains are isolated by PLLA crystalline layers, less active heterogeneities will be available for PCL crystallization, resulting in fractionated crystallization or even homogeneous nucleation.

Another important feature that can be observed in Figure 5 is that the T_g of PLLA blocks is located above or below $T_{c,PCL}$, depending on composition. This factor should also strongly affect the PCL crystallization behavior. When the PLLA content is low, PCL crystallization is scarcely confined between PLLA lamella (because PCL is the major component), and at the same time, the PLLA amorphous phase is rubbery. However, at high PLLA content, PCL crystallization is confined not only by PLLA crystal lamellae but also by PLLA vitreous amorphous phase, which in turn makes the spread of PCL crystallization from one layer to another more difficult .

Self-Nucleation of the PLLA Block. Self-nucleation experiments of the PLLA block were performed to explore its effects on the crystallization of the PCL block. Self-nucleation is expected to increase the degree of crystallinity of the PLLA block and hence the confinement of the PCL block. However, self-nucleation of the PLLA could also produce nucleation of the PCL block.

Figure 6 shows the cooling scans after self-nucleation of the PLLA block within two extreme compositions of $L_{60}C_{40}$[21] and $L_{90}C_{10}$[24], at the T_s values indicated. The degree of crystallization of the PLLA block after self-nucleation is also reported in Figure 6 enclosed in brackets. As the T_s temperature is lowered in both compositions, the PLLA block is self-nucleated, and its crystallization exotherm shifts to higher temperatures (as PLLA nucleation density increases) and increases in size. At the same time, it is clear from Figure 6a that the crystallization temperature of the PCL block within $L_{60}C_{40}$[21] shifts to higher values as the PLLA is self-nucleated and its X_c increases (decreasing T_s). Such an increase in the crystallization degree of the PLLA block increases the nucleation density available for PCL to be nucleated. A strong nucleation effect on the PCL block chains ($\Delta T \approx 12$ °C) was induced; therefore, the fractionated crystallization disappears because the isolated PCL block phase now contains the necessary self-nuclei for crystallization at lower supercoolings.

Self-nucleation experiments of PLLA block were performed for all diblock copolymers. Figure 6b,c shows DSC cooling scans after self-nucleation of PLLA block for $L_{10}C_{90}$[24]. Figure 6b,c shows only the temperature range of the PCL block and PLLA block, respectively (see legend of Figure 6). It is noteworthy that even with 10 wt % of PLLA block, an increase in crystallinity of this block (due to the self-nucleation effect revealed in Figure 6c) induces a slight nucleation of the PCL block chains ($\Delta T \approx 3$ °C). Figure 6c also showed double exothermic peaks for the PLLA block after self-nucleation at $T_s < 168$ °C; this behavior was also observed for homo-PLLA and $L_{93}C_{07}$[18] at the beginning of Domain II. Multiple exothermic peaks after self-nucleation have been explained by Fillon et al. as a consequence of entering Domain III for isotactic polypropylene.[45] Balsamo et al.[46] reported a similar behavior for a polyethylene block within a microphase-separated polystyrene-*b*-polyethylene-*b*-polycaprolactone triblock copolymer; the bimodal crystallization was explained as the result of the confined crystallization when the PE content was very low (15 wt %). The exact origin of the double exotherm observed in Figure 6c is not known and is beyond of the scope of this article.

In all diblock copolymers, a nucleation of the PCL block due to an increase in crystallinity of PLLA block was observed despite changes of $T_{g,PLLA}$. Therefore, the nucleation effect of the PCL block is generated by an increase in PLLA crystallinity (due to self-nucleation of PLLA block). It is important to highlight that although the PCL block is nucleated the highest T_c value after nucleation decreases almost linearly as PCL content decreases, so the confinement effect is still present and increases with PLLA composition.

He et al.[21] studied miscible blends of poly(butylene succinate)/poly(ethylene oxide) (PBS/PEO) where fractionated crystallization of the PEO component was observed for blends with

Table 3. Avrami Parameters for the PLLA Block Obtained by Fitting Isothermal Crystallization Data Obtained by DSC

	PLLA[24]		$L_{93}C_{07}$[18]		$L_{81}C_{19}$[21]		$L_{60}C_{40}$[21]		$L_{55}C_{45}$[18]		$L_{44}C_{56}$[25]		$L_{32}C_{68}$[22]		$L_{10}C_{90}$[24]	
T_c (°C)	n	K (min^{-n})	n	K (min^{-n})	n	K (min^{-n})	n	K (min^{-n})	n	K (min^{-n})	n	K (min^{-n})	n	K (min^{-n})	n	K (min^{-n})
105															1.99	0.1695
106															2.05	0.1322
108															2.15	0.0806
110															2.15	0.0481
113															2.42	0.0129
120	2.66	0.0888	2.66	0.0119	2.39	0.0306			2.40	0.0174	2.39	0.0067	2.60	0.0171		
121	2.68	0.0351	2.71	0.0065	2.49	0.0185	2.53	0.0175	2.61	0.0096	2.54	0.0038	2.69	0.0080		
122	2.74	0.0170	2.77	0.0039	2.51	0.0132	2.63	0.0100	2.67	0.0058	2.45	0.0035	2.75	0.0052		
123	2.87	0.0090	2.70	0.0022	2.60	0.0068	2.65	0.0059	2.44	0.0051	2.84	0.0013				
124	2.88	0.0055	2.75	0.0016	2.53	0.0053	2.66	0.0042			2.40	0.0021	2.80	0.0014		
125	2.92	0.0028	2.68	0.0008	2.77	0.0009					2.21	0.0019				
126	2.88	0.0020	2.74	0.0004	2.39	0.0306	2.74	0.0015	2.68	0.0003	2.49	0.0008	3.32	0.0001		
128	2.78	0.0006	2.69	0.0001	2.98	0.0001	2.90	0.0005	2.62	0.0002			2.69	0.0004		
130	2.60	0.0003														
132	2.47	0.0002														

PEO contents lower than 40 wt %. They also found that PEO crystallization was deeply affected by the isothermal crystallization temperature of the PBS component at intermediate PEO contents (30−50 wt %). They suggested changes in spatial distribution of PEO chains, which could be incorporated into or excluded from the interlamellar regions of PBS.[21] In our case, the PCL chains cannot be excluded from the interlamellar regions of the PLLA block because of the covalent bonds in between both blocks.

For the $L_{81}C_{19}$[21] diblock copolymer, the PCL chains also crystallized below the $T_{g,PLLA}$ and within the interlamellar regions of the previously crystallized PLLA block. So, even after self-nucleation experiments of the PLLA block, the PCL block crystallizes by homogeneous nucleation, a fact that was confirmed by Avrami analysis of isothermal crystallization data, as explained in the next section. Just two reports of homogeneous nucleation in miscible systems (such as blends) have been reported.[20,21] However, this is the first time that homogeneous nucleation is reported in miscible block copolymers, as far as the authors are aware.

Crystallization Kinetics

Homo-PLLA and PLLA Block within the PLLA-*b*-PCL Diblock Copolymers. The overall isothermal crystallization kinetics of the PLLA block within the diblock copolymers and homo-PLLA were determined by DSC experiments. The isothermal crystallization data obtained by DSC was fitted to the Avrami equation[65,66]

$$\alpha_c(t - t_0) = 1 - \exp(-K(t - t_0)^n)$$

where $\alpha_c(t - t_0)$ is the relative crystalline volume fraction of the polymer as a function of time (i.e., relative amount of material that has crystallized) and t_0 is the induction time. The parameters K and n are dependent on the nucleation type and the crystal growth geometry, K can be considered to be an overall transformation rate constant that contains contributions from both nucleation and growth, and n is the Avrami index. We performed the fitting by closely following the procedure reported in ref 66. Typical n values for polymer spherulitic crystallization are 3 and 4. An n value of 3 indicates 3D spherulitic growths from instantaneous nuclei (so-called athermal nucleation), and a value of 4 is interpreted as 3D spherulites growing from sporadic nuclei (or thermal nucleation). If the crystallization occurs in 2D aggregates (like axialites or 2D lamellar aggregates), then Avrami indexes of 2 and 3 are expected depending on whether the nucleation is instantaneous or sporadic.[65]

Crystallization kinetics of PLLA homopolymers have been analyzed in a wide temperature range by DSC and PLOM, from slightly above T_g to just below the apparent melting point.[55,59,67−74] Some peculiarities have been observed in the crystallization behavior of PLLA because it exhibits a discontinuity in the crystallization kinetics at around 100−120 °C. The crystallization rate is very high at temperatures between 100 and 120 °C, showing a clear deviation from the usual bell-shaped curve of polymer crystal growth. This discontinuity had been correlated to a transition in regimes II−III growth of spherulites,[71] to crystal polymorphism,[14,53−55,74] and to a sudden acceleration in spherulite growth rate not associated with morphological changes in the appearance of PLLA spherulite.[72]

The results of fitting the Avrami equation to the experimental data are presented in Table 3, whereas the experimentally determined inverse half-crystallization time ($1/\tau_{50\%}$) is presented in Figure 7 as a function of the crystallization temperature. The conversion range employed was 3−30%, and the correlation coefficients were always greater than 0.99. (See ref 66.) The overall crystallization rate can be approximated to $1/\tau_{50\%}$; a quantity that represents the inverse of the time needed for a particular sample to achieve 50% of the total crystallinity the material is capable of developing during the isothermal crystallization process.

This article deals only with the crystallization kinetics at temperatures >120 °C (Figure 7 and Table 3); the complex and peculiar behavior reported at temperatures < 120 °C requires further investigations.

As expected, $1/\tau_{50\%}$ correlates well with the values of the overall transformation rate (K) shown in Table 3, and they both decrease with increasing T_c. The values reported in Table 3 also revealed that in general the values of n are close to 2.5 to 3.0, indicating instantaneous spherulitic growth for compositions of PLLA higher than 32 wt %. In the case of $L_{10}C_{90}$[24] diblock copolymer, the values of n are lower and close to 2, a fact indicative of the crystallization into instantaneous 2D aggregates (like axialites or 2D lamellar aggregates). These morphologies were confirmed by PLOM experiments; see below (Figure 13).

The crystallization rates reported in Figure 7 revealed that a higher supercooling is needed to crystallize the PLLA block within $L_{10}C_{90}$[24] than homo-PLLA. The values of $1/\tau_{50\%}$ also indicate that the PLLA block within $L_{10}C_{90}$[24] crystallizes at much slower rates than homo-PLLA when similar crystallization temperatures are considered by extrapolation. To illustrate the composition dependence of the crystallization kinetics of the PLLA block within the PLLA-*b*-PCL diblock copolymers with PLLA contents higher than 10 wt %,

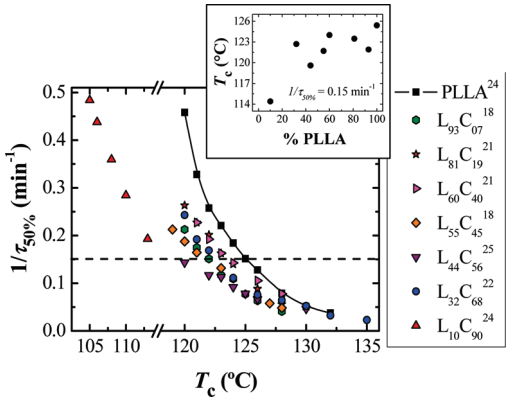

Figure 7. Inverse of half crystallization times ($1/\tau_{50\%}$) for the PLLA block within the block copolymers. Insert: Isothermal crystallization temperature (T_c) needed to obtain a value of $1/\tau_{50\%}$ = 0.15 min^{-1} (dashed line in the main figure) versus PLLA content.

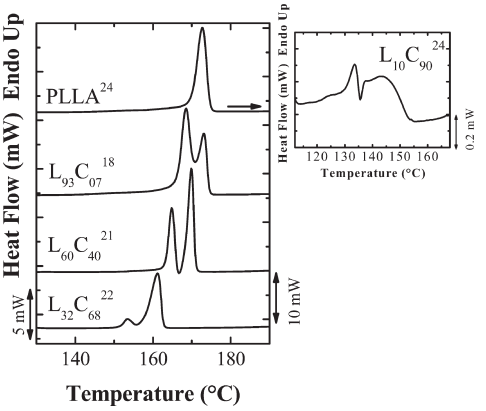

Figure 8. Subsequent heating scans (at 10 °C/min) after isothermal crystallization until saturation at 128 °C of the PLLA block within the block copolymers indicated. Insert: Subsequent heating scan after isothermal crystallization until saturation at 110 °C for the $L_{10}C_{90}^{24}$ block copolymer.

we plotted the isothermal crystallization temperature ($T_{c(0.15)}$) needed to achieve an arbitrary value of $1/\tau_{50\%}$ (i.e., 0.15 min^{-1}) (insert of Figure 7). The insert of Figure 7 shows that this isothermal crystallization temperature ($T_{c(0.15)}$) tends to decrease when the PLLA content decreases. Therefore, a higher supercooling is needed to crystallize at the same crystallization rate the PLLA block than homo-PLLA, which is a result of the diluent effect of the molten PCL chains during PLLA block crystallization. However, at higher PLLA contents, $T_{c(0.15)}$ scarcely decreases with composition but drops quickly at contents lower than 32 wt %. In summary, the effect of the molten PCL covalently bonded block was to slow down the crystallization rate of PLLA chains first slowly and then more rapidly as the content of PCL increased. Complex behaviors are revealed when comparing previous SAXS results[27,28] and DSC experiments. SAXS results evidenced a homogeneous melt for the $L_{32}C_{68}^{22}$ block copolymer, so a diluent effect of the PCL block amorphous chains is clearly expected. However, the $L_{60}C_{40}^{21}$ and $L_{44}C_{56}^{25}$ samples had heterogeneous melts with lamellar structures that were destroyed during PCL crystallization. These changes in melt structure could be the responsible for the irregular trend of PLLA crystallization kinetics with composition.

The crystallization kinetics of PLLA has been reported to be very much dependent on the molecular weight (MW). With increasing MW, the crystallization rate drops greatly.[55] The decrease in the crystallization kinetics shown in Figure 7 cannot be attributed to changes in MW (because the MW of the PLLA block is also decreasing) but to the presence of the molten PCL chains. Therefore, the decrease in crystallization rate for miscible systems can be related to a dilution effect that reduces the number of crystallizable segments on the front of the growing spherulite and also to a decrease in supercooling due to the melting point depression. Similar effects have been reported for miscible block copolymers such as polyethylene-*b*-poly(ethylene-*alt*-propylene), where a stronger dilution effect induced by amorphous poly(ethylene-*alt*-propylene) chains causes the need for much higher supercoolings to crystallize the PE block chains but at compositions close to 50 wt %.[75,76]

Heating scans performed at 10 °C/min after isothermal crystallization revealed double melting peaks for all systems except the homo-PLLA. Figure 8 shows DSC curves of the isothermally crystallized PLLA block within selected diblock copolymers at 128 °C during heating. The PLLA block of the $L_{10}C_{90}^{24}$ diblock copolymer was crystallized at 110 °C. Double melting peaks are common phenomena for polymers, especially polyesters. They have been observed for several other polyesters, such as poly(ethylene terephthalate), poly(trimethylene terephthalate), poly(butylene terephthalate), poly(3-hydroxybutyrate), and other polymers like isotactic polystyrene, poly(ether ether ketone), and poly(ether imide), to give just a few examples (refs 51, 58, 77 and references therein). The explanations for double melting include: the presence of two distinct lamellar populations, molecular weight segregation that accompanies crystallization, or the occurrence of melting-recrystallization-melting phenomena, that is, reorganization during the scan.[78] In the case of PLLA homopolymers, such double melting peaks during heating after isothermal crystallization have been reported and also evaluated.[13,49,51,52,56,58,73,77] In general, isothermally grown PLLA crystals have a large tendency to reorganize during subsequent heating scans into more stable structures through continuous partial melting/recrystallization or crystal perfection processes. For PLLA homopolymers, when crystallization is carried out at low temperatures, small crystals (i.e., thin lamellae) develop, and low values of crystallinity are attained. The large reorganization of the crystal phase results in multiple melting behavior.[51] However, just a small shoulder rather than double melting peaks was observed here for the homo-PLLA in the crystallization range of 120−140 °C, in contrast with literature reports for homopolymers of equivalent molecular weight (synthesized using zinc lactate and ethylene glycol as coinitiator and possibly other methods)[55,73] these differences could be perhaps associated with the method of synthesis that influences the nucleation process during crystallization. For the block copolymer synthesized in the same way as the homopolymers, changes in melting behavior are a direct consequence of the covalently linked PCL chains.

Figure 9 shows DSC heating scans performed at 80 °C/min after isothermal crystallization at 120 and 128 °C for selected block copolymers. It is clear from the Figure that the relative sizes of the double melting peaks change with the heating rate, as compared with Figure 8. When the scan rate is low, that is, 10 °C/min (Figure 8), there is enough time for the thin lamellae to melt and then recrystallize before melting in the second endotherm at a higher temperature; the area under the higher melting peak then corresponds to the melting of thicker crystals just formed during recrystallization.[58] Salmeron-Sánchez et al.[13] performed isothermal cold-crystallizations and explained that the low-temperature melting peak cannot be directly associated with the melting of the

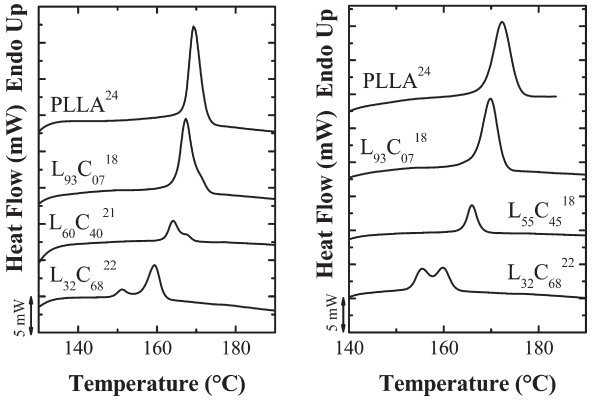

Figure 9. Subsequent heating scans at 80 °C/min after isothermal crystallization until saturation of the PLLA block within the block copolymers indicated. Left: at 120 °C. Right: at 128 °C.

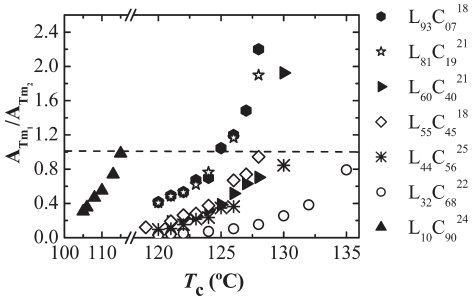

Figure 10. Ratio between the area under the lower temperature melting peak (A_{Tm1}) and the area under the higher temperature melting peak (A_{Tm2}) of the subsequent heating curves at 10 °C/min (Figure 8) after isothermal crystallization of the PLLA block within all copolymer. Dashed line indicates $A_{Tm1}/A_{Tm2} = 1$.

isothermally cold-crystallized material because fast reorganization processes take place during heating. Increasing the heating rate prevents the recrystallization phenomenon, and the high-temperature peak is hardly visible for some systems (Figure 9). It is noteworthy that although recrystallization is a relatively slow process for many polymer systems and can usually be suppressed effectively, it is not the case for PLLA-*b*-PCL with higher PCL content, where double melting peaks are still observed at 80 °C/min. For PLLA homopolymers, Salmeron-Sánchez et al.[13] reported that even at heating rates as high as 300 °C/min, the reorganization phenomena (different of recrystallization during heating) could not be hindered, causing the single temperature melting peak to be much higher than expected. However, double melting peaks due to recrystallization were not observed at heating rates > 50 °C/min.

Figure 10 shows the ratio between the area under the low-temperature melting peak (A_{Tm1}) and the area under the high-temperature melting peak (A_{Tm2}) of the heating curves at 10 °C/min after isothermal crystallization. As expected, the ratio A_{Tm1}/A_{Tm2} increases with the isothermal crystallization temperature; that is, at lower supercooling, the crystals formed are thicker (and therefore more thermodynamically stable) and therefore reorganize less during heating. Figure 10 indicates that the reorganization phenomenon of PLLA block chains within PLLA-*b*-PCL copolymers is stronger as the PCL content increases, up to 68 wt %. As the PCL block molten chains content increases, the PLLA block crystals formed during isothermal crystallization are apparently smaller, so they melt and recrystallize during heating. This result is in accordance with the presence of cold crystallization and the exothermic signal before the main melting peak during standard DSC scans. In the case of the PLLA block within $L_{10}C_{90}$[24] diblock copolymer, the reorganization process is reduced because of the lower molecular weight of the PLLA block chains. For low-molecular-weight chains, crystals tend to be more stable than that of high-molecular-weight chains crystals, and thus they tend to recrystallize less during heating.

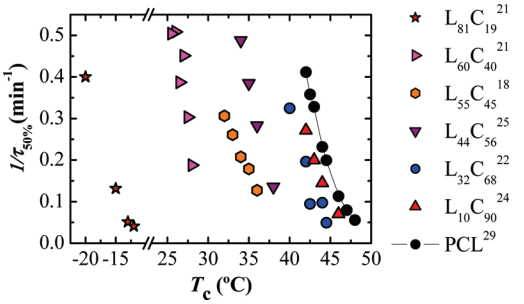

Figure 11. Inverse of half crystallization times ($1/\tau_{50\%}$) for the PCL block within the block copolymers.

Homo-PCL and PCL Block within the PLLA-*b*-PCL Diblock Copolymers. The overall crystallization rate, expressed as $1/\tau_{50\%}$ for homo-PCL and for the PCL block within the PLLA-*b*-PCL diblock copolymers, is shown in Figure 11. Isothermal crystallization of the PCL block was performed after crystallizing the PLLA block until saturation, as explained in the Experimental Section. Under this condition, the PCL block chains are nucleated by the PLLA block crystals, as revealed by the self-nucleation experiments previously shown. Also, cooling scans were performed after the PLLA block was crystallized until saturation, and it was found that $T_{c,PCL}$ shifted to higher values (results not shown).

It is clear from Figure 11 that the overall crystallization rate of the PCL block decreases with PLLA content. In addition, larger supercoolings are needed to crystallize the PCL block within the diblock copolymer as compared with the parent homopolymer. This is another evidence of the restrictions that the PCL block is facing to crystallize despite the nucleation effect produced by the PLLA block crystals. In the case of $L_{81}C_{19}$[21], the evolution of enthalpy with time was determined by ISC, following the procedure reported in ref 43. Our preceding works[27,28] showed by SAXS experiments that during isothermal PCL crystallization within the diblock copolymer with PCL contents higher than 40 wt %, rearrangements of PLLA crystal stems occurred to accommodate the previously amorphous PCL chains, disturbing the initial PLLA lamellar structure. In fact, lateral contraction of the PLLA unit cell and local melting by rearrangement of the lamellar structure was reported for $L_{60}C_{40}$[21], $L_{44}C_{56}$[25], and $L_{32}C_{68}$[22]. Although PCL crystallization effectively disturbed the previous PLLA lamellar structure (as demonstrated by SAXS experiments), it is not enough to avoid the confinement effect, as revealed by the DSC experiments performed and reported for the first time in this work. In addition, after isothermal crystallization of the PLLA block at 122 °C during SAXS experiments,[28] measured domain spacings were d = 335, 309, and 267 Å for $L_{32}C_{68}$[22], $L_{44}C_{56}$[25] and $L_{60}C_{40}$[21], respectively. In consequence, it is expected that increasing PLLA composition increases the confinement during PCL crystallization.

Figure 12 shows how the Avrami index corresponding to the crystallization of the PCL block depends on PLLA content. The Avrami index is found to decrease with PLLA content. Such a decrease can be taken as a reduction in the

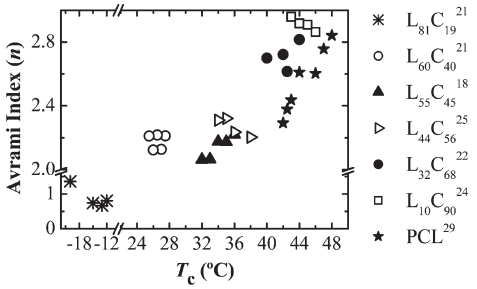

Figure 12. Avrami index values obtained by fitting isothermal crystallization data obtained by DSC for the PCL block within the block copolymers indicated.

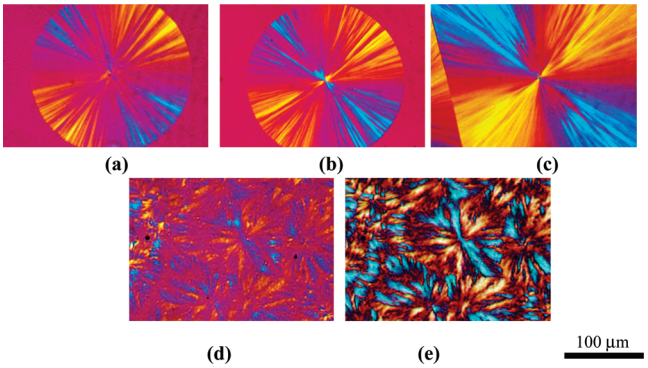

Figure 13. Polarized light optical micrographs during isothermal crystallization: (a) PLLA[24] after 8 min at 140 °C. (b) $L_{81}C_{19}$[21], after 10 min at 140 °C. (c) $L_{60}C_{40}$[21], after 30 min at 140 °C. (d) $L_{10}C_{90}$[24] after 10 min at 100 °C. (e) $L_{10}C_{90}$[24] after 3 min at 30 °C.

dimensionality growth of the PCL superstructures because more PLLA previously crystallized is present in the sample. In fact, for the $L_{81}C_{19}$[21] sample, a first-order kinetics is revealed by Avrami indexes close to 1. This result confirms that the PCL block crystallizes by homogeneous nucleation, that is, that crystal growth must be essentially instantaneous so the kinetics is entirely controlled by the nucleation process.[17,79] Values of Avrami index lower than 1 have been interpreted as being due to a nucleation process that is in between sporadic and instantaneous.[17,43] As far as we are aware, this is the first report of homogeneous nucleation of a crystallizable component within a miscible or weakly segregated diblock copolymer.

Morphology and Spherulitic Growth Rate

The morphology of the homo-PLLA and PLLA-*b*-PCL diblock copolymers was studied by PLOM. The morphologies of the PLLA-*b*-PCL diblock copolymers during isothermal crystallization at temperatures where PCL chains are molten can be observed in Figure 13 and in refs 27−29. PLLA crystallized in spherulitic morphology regardless of composition, as already reported.[27−29] Figures 13a−c shows well-defined negative PLLA spherulites, although the Maltese cross-extinction pattern tends to get blurry with increasing PCL content. (See Figure 11 from ref 28.) For the $L_{10}C_{90}$[24] block copolymer, axialite-like superstructural crystal aggregates are formed during isothermal crystallization of the PLLA block chains (Figure 13d), even though the PLLA block can only achieve a 50% crystallinity (but the sample only contains 10% of PLLA); therefore, 95% of the sample remains molten. This 2D superstructural feature (i.e., axialites) is in agreement with the Avrami index values obtained by DSC experiments, as explained in the previous section. A morphology referred to as concentric was reported by Wang et al.[80] for a two-arm star-shaped PLLA-*b*-PCL block copolymer with 28 wt % PLLA. This is in contrast with dramatic spherulitic morphology changes reported by Albuerne et al.[81] for poly(*p*-dioxanone)-*b*-poly(ε-caprolactone) (PPDX-*b*-PCL) diblock copolymers. They reported that at temperatures where both blocks crystallized, banded spherulites similar to those formed by PPDX homopolymer were clearly observed. However, at higher crystallization temperatures where the PCL block is molten, granular structures were formed if PCL was the major component. The spherulitic distortions are probably caused by the stronger segregation in between PCL and PPDX as compared with the PCL/PLLA pair.

No clear banded spherulites were observed in this work for the PLLA homopolymer and PLLA block within the diblock copolymers, as reported in the literature for PLLA homopolymers.[80,82] However, Wang and Mano[82] reported a banding-to-nonbanding morphological transition for PLLA with M_n = 86 kg/mol. The band spacing decreased with PLLA molecular weight.

PLLA templates the morphology in such a way that when the PCL block is able to crystallize at lower temperatures it has to fit in between the PLLA radially grown lamellae, and just a subtle change in the magnitude of birefringence occurs during PCL crystallization, as previously reported.[27,28] This change was more dramatic for the $L_{10}C_{90}$[24] block copolymer (Figure 13e), where a clear and intense change in the magnitude of birefringence was evident after PCL crystallization at 30 °C but without any macroscopic change in the morphology of the previously formed superstructure of the PLLA block crystals. This behavior has been previously reported for diblock copolymer with PLLA contents higher than 28 wt %.[27−29,83] However, it is surprising that even with just 10 wt % of PLLA, the axialite-like morphology is almost unchanged after crystallization of the PCL block chains; PCL chains are not confined by PLLA lamellae in this case (because of the composition, where PCL constitutes 90% by weight of the material) but are templated by them.

The radii of the homo-PLLA and the PLLA blocks spherulites increased linearly with time during isothermal crystallization experiments from the melt. The spherulitic growth rate (G) of PLLA spherulites were calculated from the slopes of the lines obtained by plotting the spherulite radius against time. Figure 14 shows the spherulitic growth rates (G) for the homo-PLLA and PLLA blocks within three diblock copolymers that possess well-separated compositions, as a function of the isothermal crystallization temperature. The insert of Figure 14 reports the isothermal crystallization temperature ($T_{c(4)}$) needed for G to reach an arbitrary value of 4 μm/min. The spherulitic growth rates are dependent on both the composition of the block copolymers and on the crystallization temperature.

Initially, increasing the PCL content in the copolymers, the bell-shaped curves of Figure 14 are slightly shifted to lower temperatures; that is, the maximum value of G shifts to lower crystallization temperatures with PCL content. In addition, the $T_{c(4)}$ values also decrease slowly initially with PCL content. Finally, for PCL contents higher than 68 wt %, the spherulitic growth rate of the PLLA block is strongly depressed as compared with homo-PLLA. Additionally, a larger shift to lower T_c of the bell-shaped curve and a significant reduction of $T_{c(4)}$ can also be observed.

The effect of the molten PCL block chains on the PLLA block spherulitic growth rate is more clearly presented in Figure 15, where G is plotted as a function of composition (in a wide composition range) at different isothermal crystallization temperatures. In general, G values decreased as the PLLA content decreases, in view of the diluent effect provoked by the PCL block molten chains, as previously explained. The dispersion of values around 120 and 130 °C are due to the shift in the maximum of the bell-shaped curves, as observed in Figure 14. The effect of molecular weight in homo-PLLA crystal growth has been evaluated in

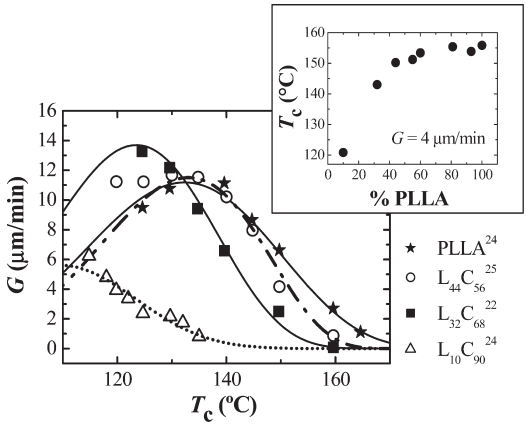

Figure 14. Spherulitic growth rate (G) of the PLLA block as a function of the isothermal crystallization temperature (T_c) for the indicated samples. Insert: Isothermal crystallization temperature (T_c) needed to achieve a fixed value of $G = 4$ μm/min versus PLLA content.

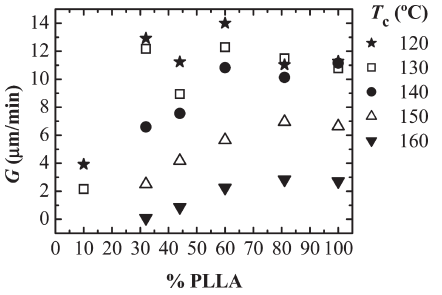

Figure 15. Spherulitic growth rate (G) of the PLLA block within all copolymers as a function of PLLA content at the isothermal crystallization temperatures (T_c) indicated.

a molecular weight range of 5−690 kg/mol.[55,61,68,69,71] The spherulitic growth rate of PLLA crystals formed at identical temperatures decreased as the molecular weight increased. However in PLLA-*b*-PCL diblock copolymers, this effect is once more overwhelmed by the presence of the molten PCL chains. It is noteworthy that for more strongly segregated systems (but still weakly segregated) as PPDX-*b*-PCL, the spherulitic growth rate of the PPDX block was an order of magnitude lower than that of neat PPDX within block copolymers with only 23 wt % of molten PCL.[84] These results suggest that despite the diluent effect (caused by miscibility) or melt structure (for weakly segregated systems), PLLA crystallization kinetics and spherulitic growth rate (within PLLA-*b*-PCL block copolymers) are not significantly disturbed at crystallization temperatures >120 °C until the PCL content reaches 90 wt %.

Conclusions

We have investigated the crystallization kinetics and morphology of PLLA and PCL blocks within a series of PLLA-*b*-PCL double crystalline diblock copolymers. In general, both T_c and T_m of PLLA blocks are depressed with PCL content because of a diluent effect, caused by the miscibility or partial miscibility of both phases. The crystallization kinetics of the PLLA blocks slightly decreases as compared with the parent homopolymer but weakly varies with composition except for contents lower than 10 wt %. An Avrami analysis of the data indicated that 3D superstructures were formed from instantaneous nuclei ($n = 2.5$ to 3) except for $L_{10}C_{90}$[24], where values close to 2 were obtained, an indication of the formation of instantaneously nucleated axialites. This was confirmed by the observation of spherulites in PLOM. Even at contents as low as 5 wt % of crystallizable chains in $L_{10}C_{90}$[24], PLLA crystallizes in superstructures like axialites observed by PLOM and predicted by Avrami analysis.

Heating scans (performed at 10 °C/min) after isothermal crystallization show double melting peaks of the PLLA block that were attributed to reorganization processes during the scan, but these were not observed for the PLLA homopolymer. These reorganization processes were confirmed by performing heating scans at 80 °C/min, where the relative size of the double melting peaks changed with the heating rate. However, even at this rate the reorganization cannot be suppressed completely for some compositions. The ratio between the area of both the lower and higher melting peaks indicated that the reorganization phenomena increases with PCL content, except for the $L_{10}C_{90}$[24] sample.

Spherulitic growth rates also changed with PCL content. Bell-shaped curves were obtained, and the maximum peaks were slightly shifted to lower crystallization temperatures. G and T_c values decreased with decreasing PLLA composition at the same crystallization temperatures or constant G value, respectively, because of the diluent effect.

The PCL block behaved in a different way when it was subsequently crystallized after PLLA crystallization. It crystallized within the interlamellar regions of the previously formed PLLA block spherulites; therefore, fractionated crystallization occurred for PCL contents lower than 40 wt %. A homogeneous nucleation process was revealed and confirmed by Avrami analysis ($n \approx 1$) for the PCL block within the $L_{81}C_{19}$[21] sample. The fractionated crystallization was related to the topological restrictions caused by the covalently linked PLLA block that was previously crystallized. For PCL contents lower than 40 wt %, the $T_{g,PLLA}$ values are close to or higher than the crystallization temperature of the PCL blocks, which is expected to increase the topological restrictions during PCL crystallization. For PCL contents lower than 7 wt %, the PCL chains did not crystallize.

Another interesting behavior revealed for this complex system was a nucleation effect induced by PLLA crystals previously formed during self-nucleation experiments on the PCL block. This nucleation effect was dependent on the degree of crystallization of the PLLA block. Despite that, the crystallization kinetics of the PCL block was significantly reduced, even more than for the PLLA block. The crystallization and morphology of the biodegradable polymers PLLA and PCL can be strongly influenced by coupling them in double-crystalline diblock copolymers, a fact that will also influence their performance in possible biomedical applications.

Acknowledgment. CIRMAP thanks the Belgian Federal Government Office of Science Policy (STC-PAI 6/27) and Cécile Delcourt for her efficient help in the synthesis and molecular characterization of the diblock copolymers. J-M.R. is "chargé de recherché" by the F.R.S.-FNRS.

References and Notes

(1) Nair, L. S.; Laurencin, C. T. *Prog. Polym. Sci.* **2007**, *32*, 762–798.
(2) Garlotta, D. *J. Polym. Environ.* **2002**, *9*, 63–84.
(3) Pappalardo, D.; Annunziata, L.; Pellecchia, C. *Macromolecules* **2009**, *42*, 6056–6062.
(4) Ghoroghchian, P. P.; Li, G.; Levine, D. H.; Davis, K. P.; Bates, F. S.; Hammer, D. A.; Therien, M. J. *Macromolecules* **2006**, *39*, 1673–1675.
(5) Zhou, S.; Deng, X.; Yang, H. *Biomaterials* **2003**, *24*, 3563–3570.
(6) Sinha, V. R.; Bansal, K.; Kaushik, R.; Kumria, R.; Trehan, A. *Int. J. Pharm.* **2004**, *278*, 1–23 and references therein.
(7) Dell'Erba, R.; Groeninckx, G.; Maglio, G.; Malinconico, M.; Migliozzi, A. *Polymer* **2001**, *42*, 7831–7840.
(8) Na, Y.-H.; He, Y.; Shuai, X.; Kikkawa, Y.; Doi, Y.; Inoue, Y. *Biomacromolecules* **2002**, *3*, 1179–1186.
(9) Yang, J. M.; Chen, H. L.; You, J. W.; Hwang, J. C. *Polym. J.* **1997**, *29*, 657–662.

(10) Sakai, F.; Nishikawa, K.; Inoue, Y.; Yazawa, K. *Macromolecules* **2009**, *21*, 8335–8342.
(11) Hamley, I. W. *The Physics of Block Copolymers*; Oxford University Press: Oxford, U.K., 1998.
(12) Castillo, R. V.; Müller, A. J. *Prog. Polym. Sci.* **2009**, *34*, 516–560.
(13) Salmerón-Sanchez, M.; Mathot, V. B. F.; Vanden Poel, G.; Gómez Ribelles, J. L. *Macromolecules* **2007**, *40*, 7989–7997.
(14) Kawai, T.; Rahman, N.; Matsuba, G.; Nishida, K.; Kanaya, T.; Nakano, M.; Okamoto, H.; Kawada, J.; Usuki, A.; Honma, N.; Nakajima, K.; Matsuda, M. *Macromolecules* **2007**, *40*, 9463–9469.
(15) Hamley, I. W. *Adv. Polym. Sci.* **1999**, *148*, 113–137.
(16) Loo, Y. L.; Register, R. A. Crystallization within Block Copolymer Mesophases. In *Developments in Block Copolymer Science and Technology*; Hamley, I. W., Ed.; Wiley: New York, 2004.
(17) Müller, A. J.; Balsamo, V.; Arnal, M. L. *Adv. Polym. Sci.* **2005**, *190*, 1–63.
(18) Müller, A. J.; Balsamo, V.; Arnal, M. L. Crystallization in Block Copolymers with More than One Crystallizable Block. In *Lecture Notes in Physics: Progress in Understanding of Polymer Crystallization*; Reiter, G, Strobl, G, Eds.; Springer: Berlin, 2007.
(19) Nandan, B.; Hsu, J.-Y.; Chen, H.-L. *Polymer Rev.* **2007**, *46*, 143–172.
(20) He, Y.; Zhu, B.; Kai, W.; Inoue, Y. *Macromolecules* **2004**, *37*, 3337–3345.
(21) He, Y.; Zhu, B.; Kai, W.; Inoue, Y. *Macromolecules* **2004**, *37*, 8050–8056.
(22) Zhao, L.; Kai, W.; He, Y.; Zhu, B.; Inoue, Y. *J. Polym. Sci., Part B: Polym. Phys.* **2005**, *43*, 2665–2676.
(23) Maglio, G.; Migliozzi, A.; Palumbo, R. *Polymer* **2003**, *44*, 369–375.
(24) Kim, J. K.; Park, D.-J.; Lee, M.-S.; Ihn, K. J. *Polymer* **2001**, *42*, 7429–7441.
(25) Ho, R.-M.; Hsieh, P.-Y.; Tseng, W.-H.; Lin, C.-C.; Huang, B.-H.; Lotz, B. *Macromolecules* **2003**, *36*, 9085–9092.
(26) Jeon, O.; Lee, S.-H.; Kim, S. H.; Lee, Y. M.; Kim, Y. H. *Macromolecules* **2003**, *36*, 5585–5592.
(27) Hamley, I. W.; Castelletto, V.; Castillo, R. V.; Müller, A. J.; Martin, C. M.; Pollet, E.; Dubois, Ph. *Macromolecules* **2005**, *38*, 463–472.
(28) Hamley, I. W.; Parras, P.; Castelletto, V.; Castillo, R. V.; Müller, A. J.; Pollet, E.; Dubois, Ph.; Martin, C. M. *Macromol. Chem. Phys.* **2006**, *207*, 941–953.
(29) Laredo, E.; Prutsky, N.; Bello, A.; Grimau, M.; Castillo, R. V.; Müller, A. J.; Dubois, Ph. *Eur. Phys. J.* **2007**, *E23*, 295–303.
(30) Qian, H.; Bei, J.; Wang, S. *Polym. Degrad. Stab.* **2000**, *68*, 423–429.
(31) Wei, M.; Shuai, X.; Tonelli, A. E. *Biomacromolecules* **2003**, *4*, 783–792.
(32) Huang, M.- H.; Li, S.; Vert, M. *Polymer* **2004**, *45*, 8675–8681.
(33) Piao, L.; Sun, J.; Zhong, Z.; Liang, Q.; Chen, X.; Kim, J.-H.; Jing, X. *J. Appl. Polym. Sci.* **2006**, *102*, 2654–2660.
(34) Porbeni, F. E.; Shin, I. D.; Shuai, X.; Wang, X.; White, J. L.; Jia, X.; Tonelli, A. E. *J. Polym. Sci., Part B: Polym. Phys.* **2005**, *43*, 2086–2096.
(35) Hiljanen-Vainio, M.; Karjalainen, T.; Seppälä, J. *J. Appl. Polym. Sci.* **1996**, *59*, 1281–1288.
(36) Sun, J.; Chen, X.; He, C.; Jing, X. *Macromolecules* **2006**, *39*, 3717–3719.
(37) Yang, J.; Zhao, T.; Zhou, Y.; Liu, L.; Li, G.; Zhou, E.; Chen, X. *Macromolecules* **2007**, *40*, 2791–2797.
(38) Shuai, X.; Porbeni, F. E.; Wei, M.; Shin, D.; Tonelli, A. E. *Macromolecules* **2001**, *34*, 7355–7361.
(39) Li, J.; Li, X.; Ni, A.; Leong, K. W. *Macromolecules* **2003**, *36*, 2661–2667.
(40) Li, L.; Zhong, Z.; De Jeu, W. H.; Dijkstra, P. J.; Feijen, J. *Macromolecules* **2004**, *37*, 8641–8646.
(41) Huang, S.; Jiang, S.; Chen, X.; An, L. *Langmuir* **2009**, *25*, 13125–13132.
(42) Jacobs, C.; Dubois, Ph; Jerome, R.; Teyssie, Ph. *Macromolecules* **1991**, *24*, 3027–3034.
(43) Balsamo, V.; Urdaneta, N.; Pérez, L.; Carrizales, P.; Abetz, V.; Müller, A. J. *Eur. Polym. J.* **2004**, *40*, 1033–1049.
(44) Pijpers, T. F. J.; Mathot, V. B. F.; Goderis, B.; Scherrenberg, R. L.; van der Vegte, E. W. *Macromolecules* **2002**, *35*, 3601–3613.
(45) Fillon, B.; Wittman, J. C.; Lotz, B.; Thierry, A. *J. Polym. Sci., Part B* **1993**, *31*, 1383–1393.
(46) Müller, A. J.; Balsamo, V.; Arnal, M. L.; Jakob, T.; Schmalz, H.; Abetz, V. *Macromolecules* **2002**, *35*, 3048–3058.
(47) Lorenzo, A. T.; Arnal, M. L.; Sánchez, J. J.; Müller, A. J. *J. Polym. Sci., Part B: Polym. Phys.* **2006**, *44*, 1738–1750.
(48) Müller, A. J.; Arnal, M. L. *Prog. Polym. Sci.* **2005**, *30*, 559–603.
(49) Wang, Y.; Mano, J. F. *Eur. Polym. J.* **2005**, *41*, 2335–2342.
(50) Wang, Y.; Mano, J. F. *J. Therm. Anal. Cal.* **2005**, *80*, 171–175.
(51) Di Lorenzo, M. L. *J. Appl. Polym. Sci.* **2006**, *100*, 3145–3151.
(52) Zhang, J.; Tashiro, K.; Tsuji, H.; Domb, A. J. *Macromolecules* **2008**, *41*, 1352–1357.
(53) Zhang, J.; Duan, Y.; Sato, H.; Tsuji, H.; Noda, I.; Yan, S.; Ozaki, Y. *Macromolecules* **2005**, *38*, 8012–8021.
(54) Ohtani, Y.; Okumura, K.; Kawaguchi, A. *J. Macromol. Sci., Part B: Phys.* **2003**, *3*−*4*, 875–888.
(55) Pan, P.; Kai, W.; Zhu, B.; Dong, T.; Inoue, Y. *Macromolecules* **2007**, *40*, 6898–6905.
(56) Yasuniwa, M.; Sakamo, K.; Ono, Y.; Kawahara, W. *Polymer* **2008**, *49*, 1943–1951.
(57) Pan, P.; Inoue, Y. *Prog. Polym. Sci.* **2009**, *34*, 605–640.
(58) Sarasua, J.-R.; Prud'homme, R. E.; Wisniewski, M.; Le Borgne, A.; Spassky, N. *Macromolecules* **1998**, *31*, 3895–3905.
(59) Iannace, S.; Nicolais, L. *J. Appl. Polym. Sci.* **1997**, *64*, 911–919.
(60) Tsuji, H.; Tezuka, Y. *Biomacromolecules* **2004**, *5*, 1181–1186.
(61) Tsuji, H.; Miyase, T.; Tezuka, Y.; Saha, S. K. *Biomacromolecules* **2005**, *6*, 244–254.
(62) Sun, J.; Hong, Z.; Yang, L.; Tang, Z.; Chen, X.; Jing, X. *Polymer* **2004**, *45*, 5969–5977.
(63) Shin, D.; Shin, K.; Aamer, K. A.; Tew, G. N.; Russell, T. P.; Lee, J. H.; Jho, J. Y. *Macromolecules* **2005**, *38*, 104–109.
(64) Cai, C.; Wang, L.; Dong, C.-M. *J. Polym. Sci., Part A: Polym. Chem.* **2006**, *44*, 2034–2044.
(65) Gedde, U. W. *Polymer Physics*; Chapman and Hall: London, 1995.
(66) Lorenzo, A. T.; Arnal, M. L.; Albuerne, J.; Müller, A. J. *Polym. Test.* **2007**, *26*, 222–231.
(67) Marega, C.; Marigo, A.; Di Noto, V.; Zannetti, R. *Makromol. Chem.* **1992**, *193*, 1599–1606.
(68) Vasanthakumari, R.; Pennings, A. J. *Polymer* **1983**, *24*, 175.
(69) Miyata, T.; Masuko, T. *Polymer* **1998**, *39*, 5515–5521.
(70) Di Lorenzo, M. L. *Eur. Polym. J.* **2001**, *42*, 9441–9446.
(71) Abe, H.; Kikkawa, Y.; Inoue, Y.; Doi, Y. *Biomacromolecules* **2001**, *2*, 1007–1014.
(72) Di Lorenzo, M. L. *Eur. Polym. J.* **2005**, *41*, 569–575.
(73) He, Y.; Fan, Z.; Hu, Y.; Wu, T.; Wei, J.; Li, S. *Eur. Polym. J.* **2007**, *43*, 4431–4439.
(74) Pan, P.; Zhu, B.; Kai, W; Dong, T.; Inoue, Y. *J. Appl. Polym. Sci.* **2008**, *107*, 54–62.
(75) Lorenzo, A. T.; Arnal, M. L.; Müller, A. J.; Boschetti-de-Fierro, A.; Abetz, V. *Eur. Polym. J.* **2006**, *42*, 516–533.
(76) Müller, A. J.; Lorenzo, A. T.; Arnal, M. L.; Boschetti-de-Fierro, A.; Abetz, V. *Macromol. Symp.* **2006**, *240*, 114–123.
(77) Shieh, Y.-T.; Liu, G.-L. *J. Polym. Sci., Part B: Polym. Phys.* **2007**, *45*, 466–474.
(78) Wunderlich, B. *Macromolecular Physics: Crystal Melting*; Academic Press: New York, 1980; Vol. *3*.
(79) Loo, Y. L.; Register, R. A.; Ryan, A. J.; Dee, G. T. *Macromolecules* **2001**, *34*, 7973–7982.
(80) Wang, Y.; Funar, S. S.; Mano, J. F. *Macromol. Chem. Phys.* **2006**, *207*, 1262–1271.
(81) Albuerne, J.; Marquez, L.; Müller, A. J.; Raquez, J. M.; Degee, Ph.; Dubois, Ph.; Castelletto, V.; Hamley, I. *Macromolecules* **2003**, *36*, 1633–1644.
(82) Wang, Y.; Mano, J. F. *J. Appl. Polym. Sci.* **2007**, *105*, 3500–3504.
(83) Wang, J.-L.; Dong, C.-M. *Macromol. Chem. Phys.* **2006**, *207*, 554–62.
(84) Müller, A. J.; Albuerne, J.; Márquez, L.; Raquez, J. M.; Degée, Ph.; Dubois, Ph.; Hobbs, J.; Hamley, I. W. *Faraday Discuss.* **2005**, *128*, 231–252.